eLIFE elifesciences.org

RESEARCH ARTICLE

Figures and figure supplements

Defective synaptic transmission causes disease signs in a mouse model of juvenile neuronal ceroid lipofuscinosis

Benedikt Grünewald *et al*

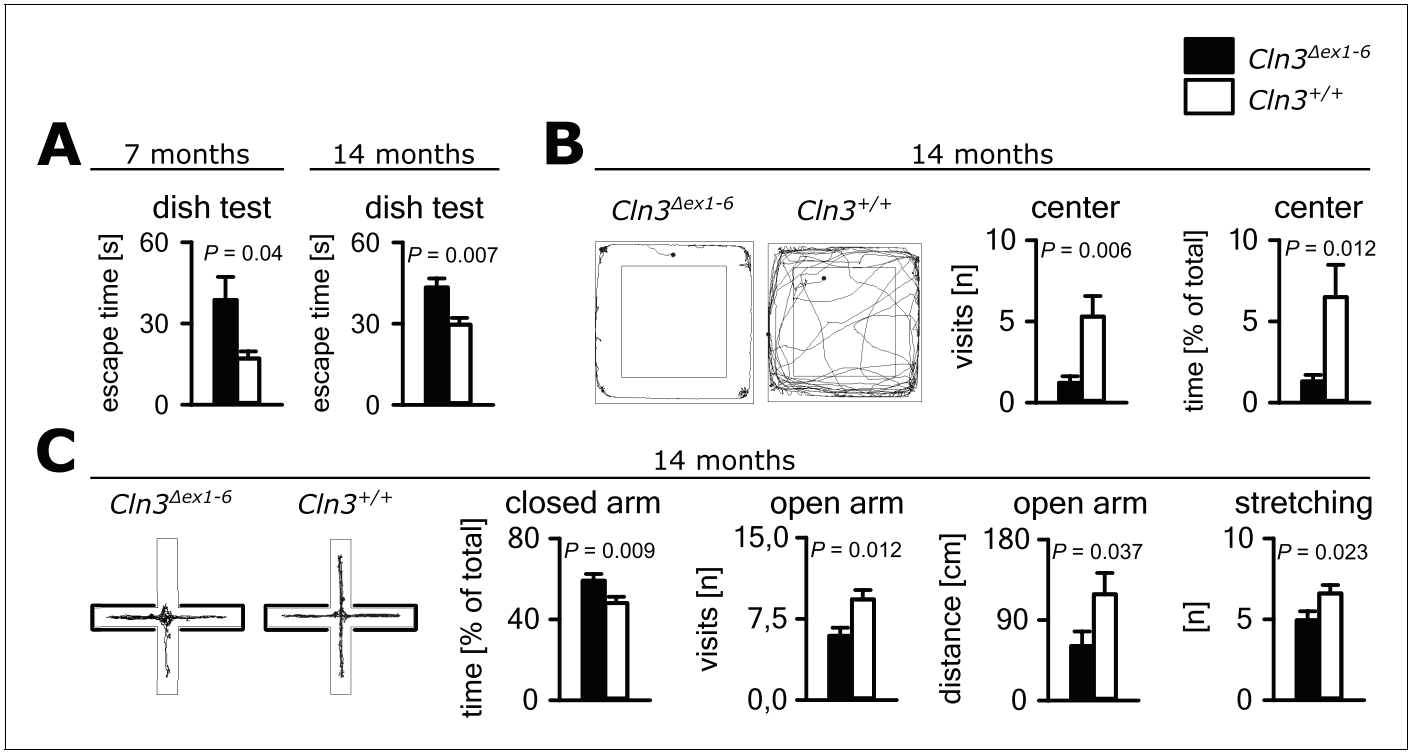

Figure 1. Anxiety-related behavior in *Cln3*$^{\Delta ex1-6}$ mice. (**A**) Escape time to cross the rim barrier of a petri dish was increased in *Cln3*$^{\Delta ex1-6}$ mice compared to wt littermates indicating reduced explorative behavior (wt: *n* = 15/24 [7 month/14 month]; Cln3$^{\Delta ex1-6}$: *n* = 14/18; Mann-Whitney Test). (**B**) Increased anxiety-related behavior of *Cln3*$^{\Delta ex1-6}$ mice at the age of 14 months in the open field (OF) test. Representative tracks and data plots for OF related to genotypes. Note that *Cln3*$^{\Delta ex1-6}$ mice visited the center area in the OF less frequently and spent more time in the peripheral areas (n = 18 vs. 20; Mann-Whitney test). (**C**) Increased anxiety-related behavior in the elevated plus maze (EPM) test at the age of 14 months. In the EPM *Cln3*$^{\Delta ex1-6}$ mice showed less visits and reduced travel distance in the open arms and preferred to stay in the closed arms indicating increased anxiety-related behavior. Microbehavior analysis revealed reduced stretchings confirming reduced explorative drive in both test paradigms (n = 18 vs. 20; open arm distance: Mann-Whitney, all other Student's t-test). Exact values of N, dispersion and precision measures are provided in ***Supplementary file 2***.

DOI: https://doi.org/10.7554/eLife.28685.002

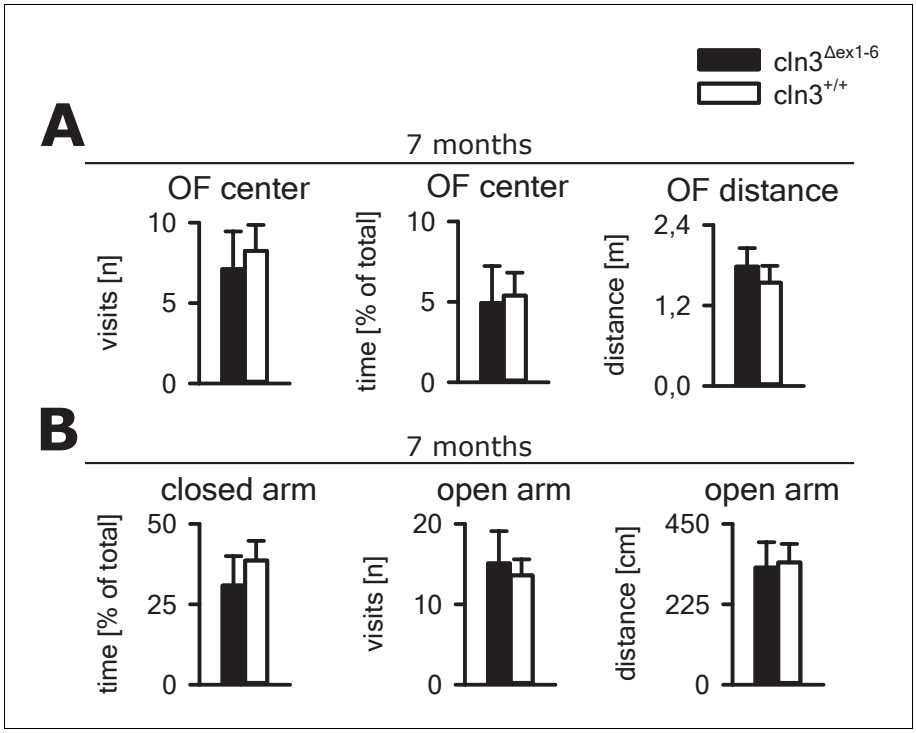

Figure 1—figure supplement 1. Open field (OF) and elevated plus maze testing at the age of 7 months. (**A**) Center visits and total movement of $Cln3^{\Delta ex1-6}$ mice during free exploration in the OF maze were unchanged in comparison to wt littermates at the age of 7 months (*n* = 9 vs 8; OF visits and OF distance: Student´s t-test; OF center time: Mann-Whitney test). (**B**) In the elevated plus maze, there was no evidence for increased anxiety-related behavior and disturbed walking distance at the age of 7 months (*n* = 9 vs 8; Student's test). Exact dispersion and precision measures are provided in ***Supplementary file 2***.

DOI: https://doi.org/10.7554/eLife.28685.003

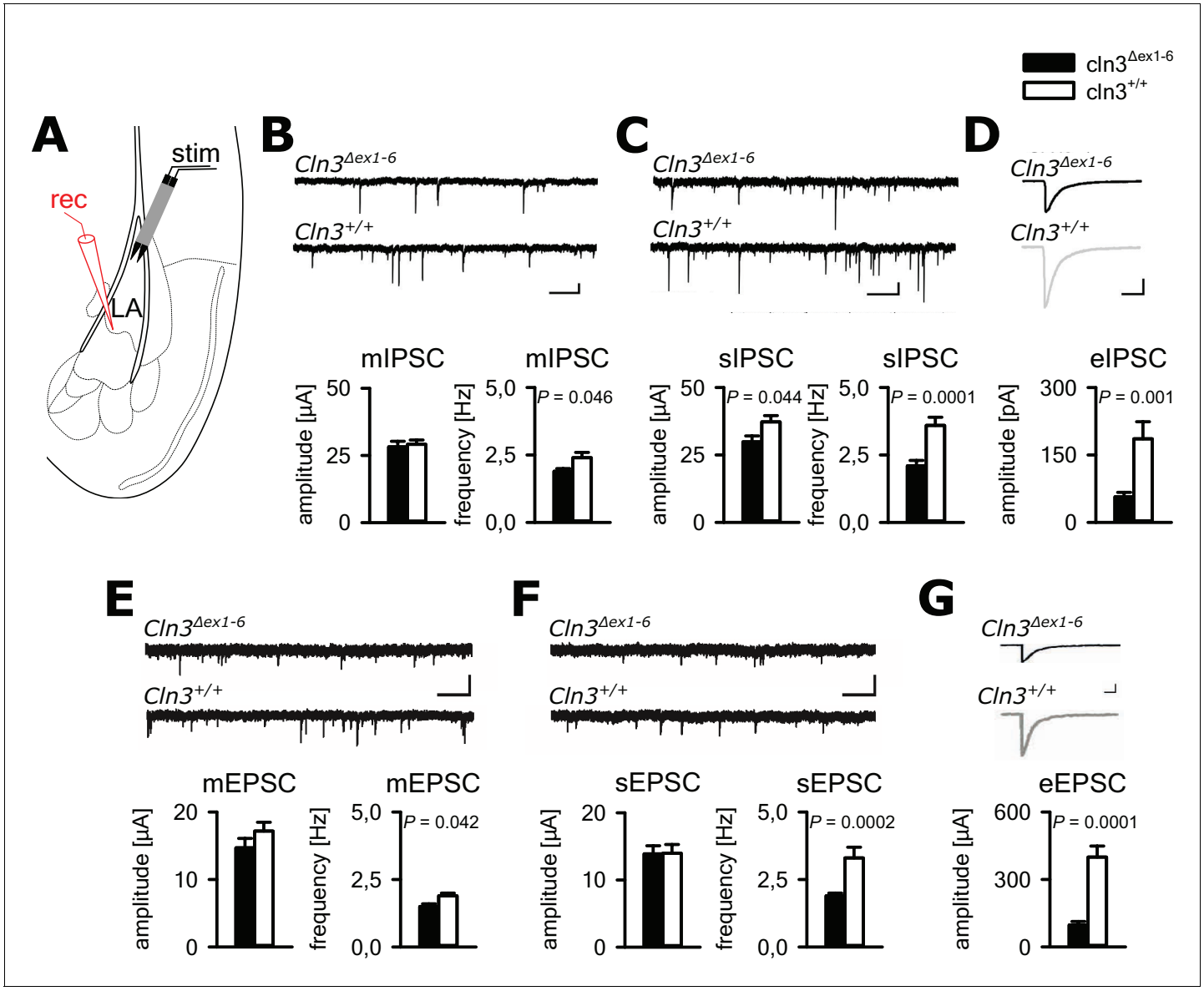

Figure 2. Defective synaptic transmission in the amygdala of 14 months old *Cln3*$^{\Delta ex1-6}$mice. (**A**) Schematic illustration of the recording situation in the lateral amygdala (LA). Whole-cell patch recordings were performed from principal neurons (PN) in the LA (rec) by local stimulation of GABAergic or glutamatergic afferences (stim). (**B**) The frequency of GABAergic miniature inhibitory postsynaptic currents (mIPSC) in LA PNs was significantly reduced in Cln3$^{\Delta ex1-6}$ mice, whereas mean amplitude was unchanged (wt: *n* = 27/7 [number of recordings/number of mice]; *Cln3*$^{\Delta ex1-6}$: *n* = 32/7; Student's t-test; scale bars 100 pA and 50 ms). (**C**) The frequency and the amplitude of spontaneous (s) IPSC were reduced in Cln3$^{\Delta ex1-6}$ mice (wt: *n* = 33/7; *Cln3*$^{\Delta ex1-6}$: *n* = 33/7; Student's t-test). (**D**) After extracellular microstimulation of GABAergic afferents, peak amplitude of evoked IPSC in amygdala PNs was reduced (wt: *n* = 25/7; *Cln3*$^{\Delta ex1-6}$: *n* = 28/7; Student's t-test). (**E**) The frequency of miniature excitatory postsynaptic currents (mESPC) was reduced in *Cln3*$^{\Delta ex1-6}$ mice (wt: *n* = 23/6; *Cln3*$^{\Delta ex1-6}$: *n* = 27/7; Student's t-test; scale bars 20 pA and 500 ms). (**F**) The frequency of the spontaneous (s) EPSC was reduced while the mean amplitude was unaffected (wt; *n* = 27/6; *Cln3*$^{\Delta ex1-6}$; *n* = 33/7; Student's t-test; scale bars 20 pA and 500 ms). (**G**) The amplitude of evoked (e) EPSC was reduced in *Cln3*$^{\Delta ex1-6}$ mice (wt: *n* = 23/6; *Cln3*$^{\Delta ex1-6}$: *n* = 24/7; Student's t-test; scale bars 100 pA and 500 ms). Exact values of N, dispersion and precision measures are provided in ***Supplementary file 2***.

DOI: https://doi.org/10.7554/eLife.28685.004

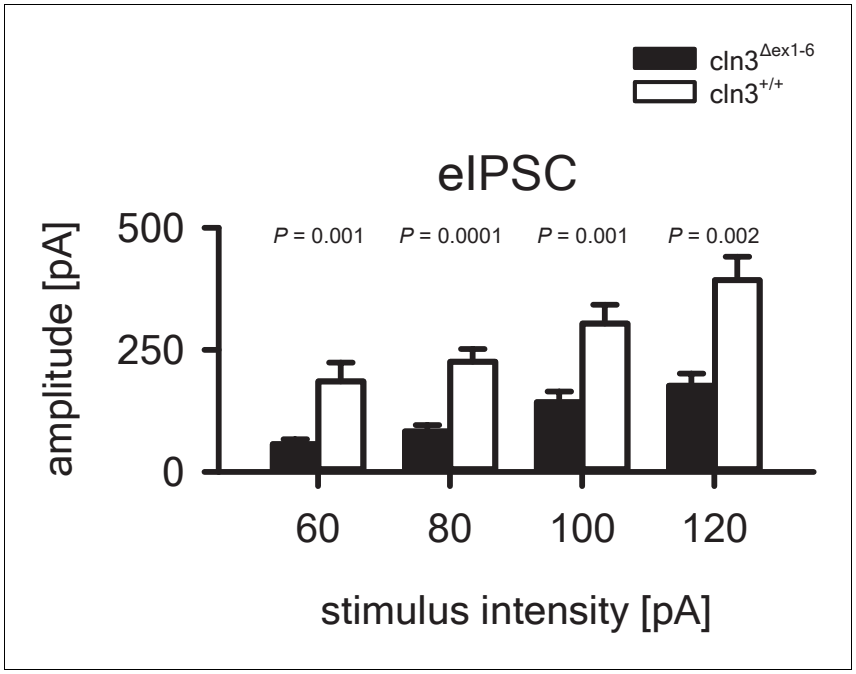

Figure 2—figure supplement 1. In-out curve showing reduced eIPSC in the amygdala of *Cln3*$^{\Delta ex1\text{-}6}$ mice at the age of 14 months. The amplitude of eIPSCs in *Cln3*$^{\Delta ex1\text{-}6}$ mice is reduced at all stimulation intensities that were tested (wt: n = 25/7 (number of recordings/number of mice); *Cln3*$^{\Delta ex1\text{-}6}$: *n* = 28/7; Student's t-test). Exact values of N, dispersion and precision measures are provided in ***Supplementary file 2***.

DOI: https://doi.org/10.7554/eLife.28685.005

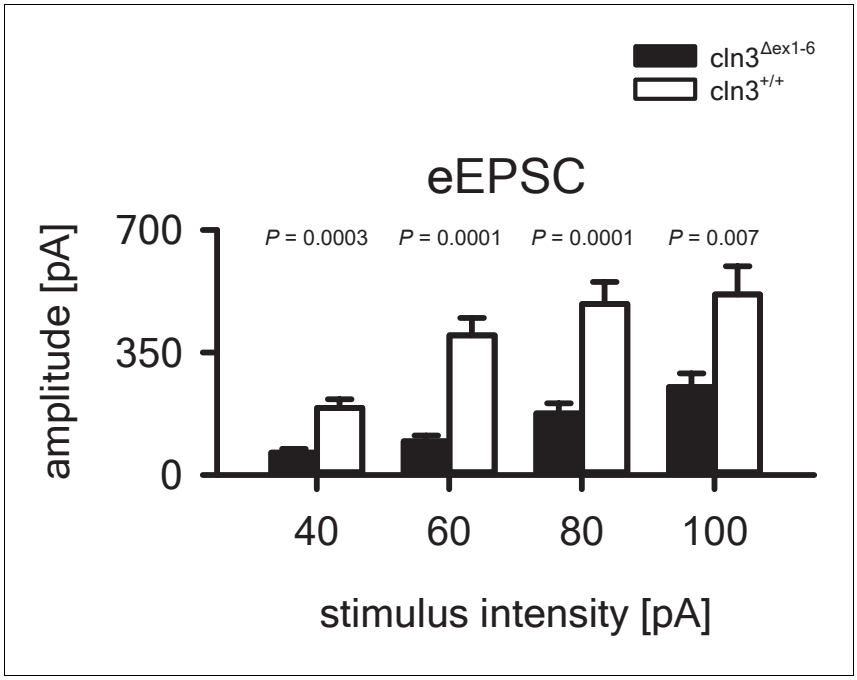

Figure 2—figure supplement 2. In-out curve showing reduced eEPSC in the amygdala of 14-month-old *Cln3*$^{\Delta ex1-6}$ mice. eEPSC amplitude is reduced in *Cln3*$^{\Delta ex1-6}$ mice at all stimulation intensities that were tested (23/6 vs. 24/7; Student's t-test. Exact values of N, dispersion and precision measures are provided in ***Supplementary file 2***.
DOI: https://doi.org/10.7554/eLife.28685.006

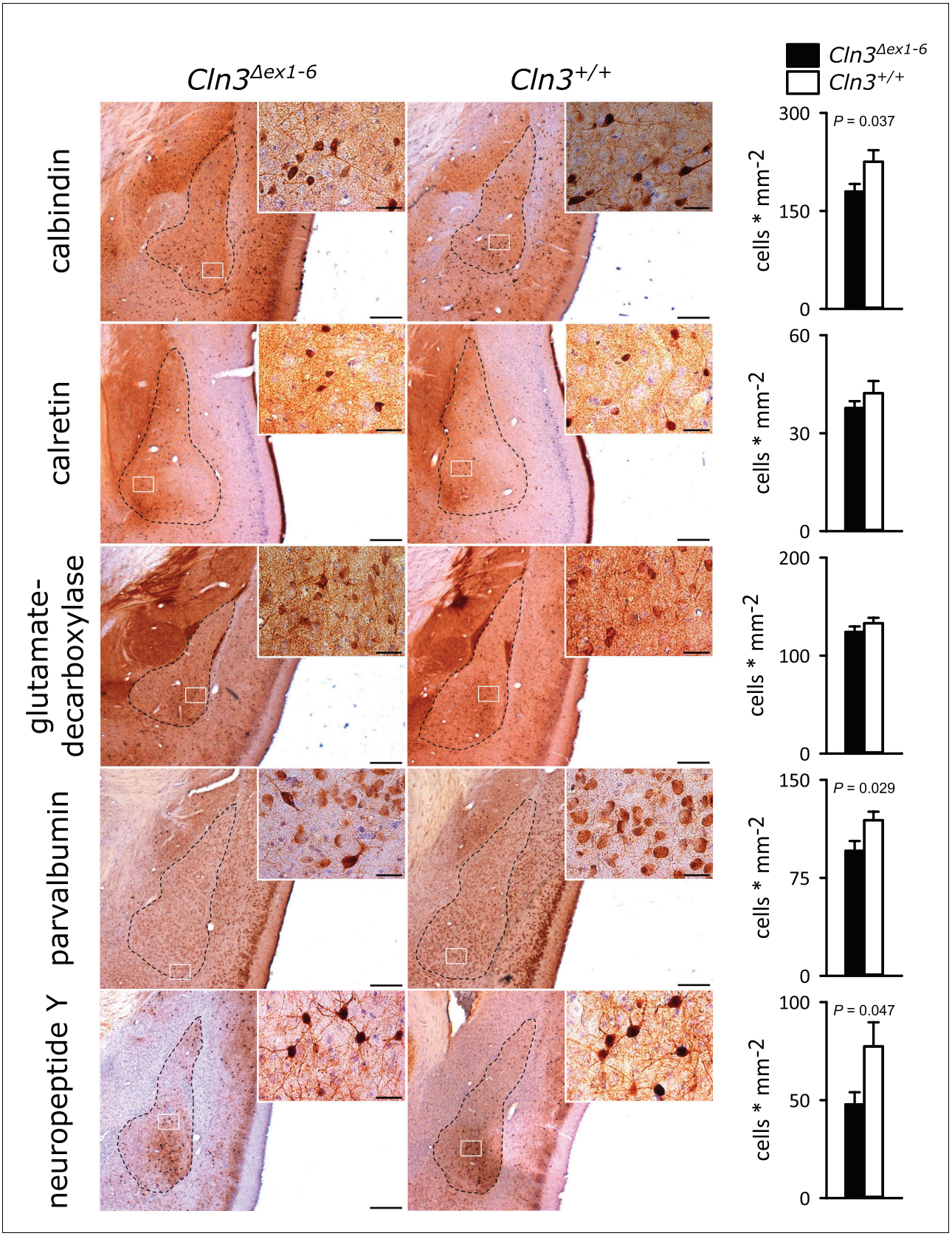

Figure 3. Loss of GABAergic interneurons in the amygdala of *Cln3*$^{\Delta ex1-6}$ mice at the age of 14 months. In coronar brain slices the area of the amygdala core regions was morphologically identified by their characteristic shape and distribution of neuronal nuclei (dashed lines). Interneuron subtypes were

Figure 3 continued on next page

Figure 3 continued

differentiated using immunohistological stains for the respective antigens. Note that in 14-month-old *Cln3*$^{\Delta ex1\text{-}6}$ mice the number of calbindin, parvalbumin, and neuropeptide Y positive interneurons in the amygdala area was reduced compared to age-matched wt littermates, whereas other markers were unchanged (scale bar: 500 μm; inset: 50 μm; *n = 13 to 16*, Mann-Whitney test). Exact values of N, dispersion and precision measures are provided in ***Supplementary file 2***.

DOI: https://doi.org/10.7554/eLife.28685.007

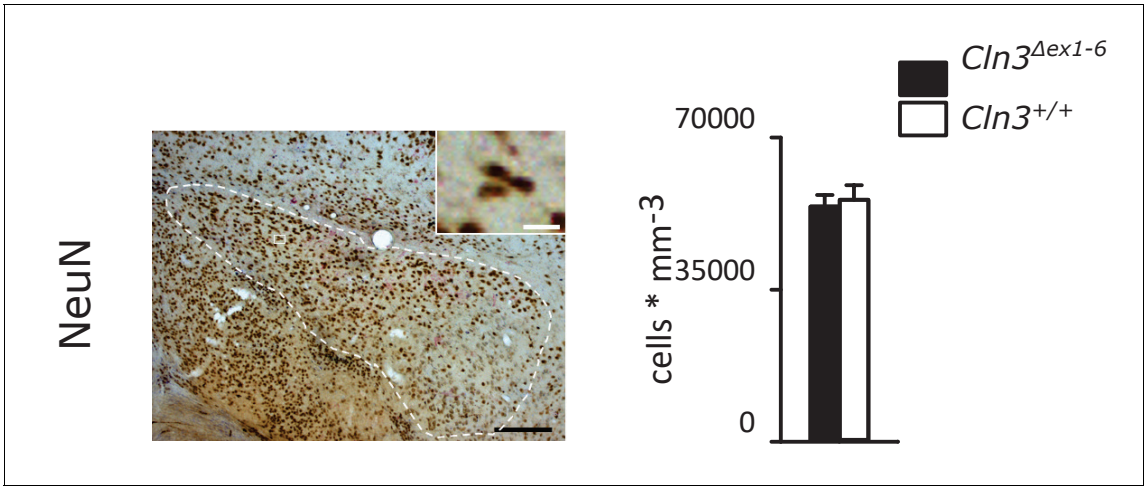

Figure 3—figure supplement 1. Density of NeuN-positive cells is unchanged in the amygdala of 14-month-old C*ln3*$^{\Delta ex1\text{-}6}$ mice (n = 9 vs. 8). Exact p values as well as exact dispersion and precision measures are provided in ***Supplementary file 2***.

DOI: https://doi.org/10.7554/eLife.28685.008

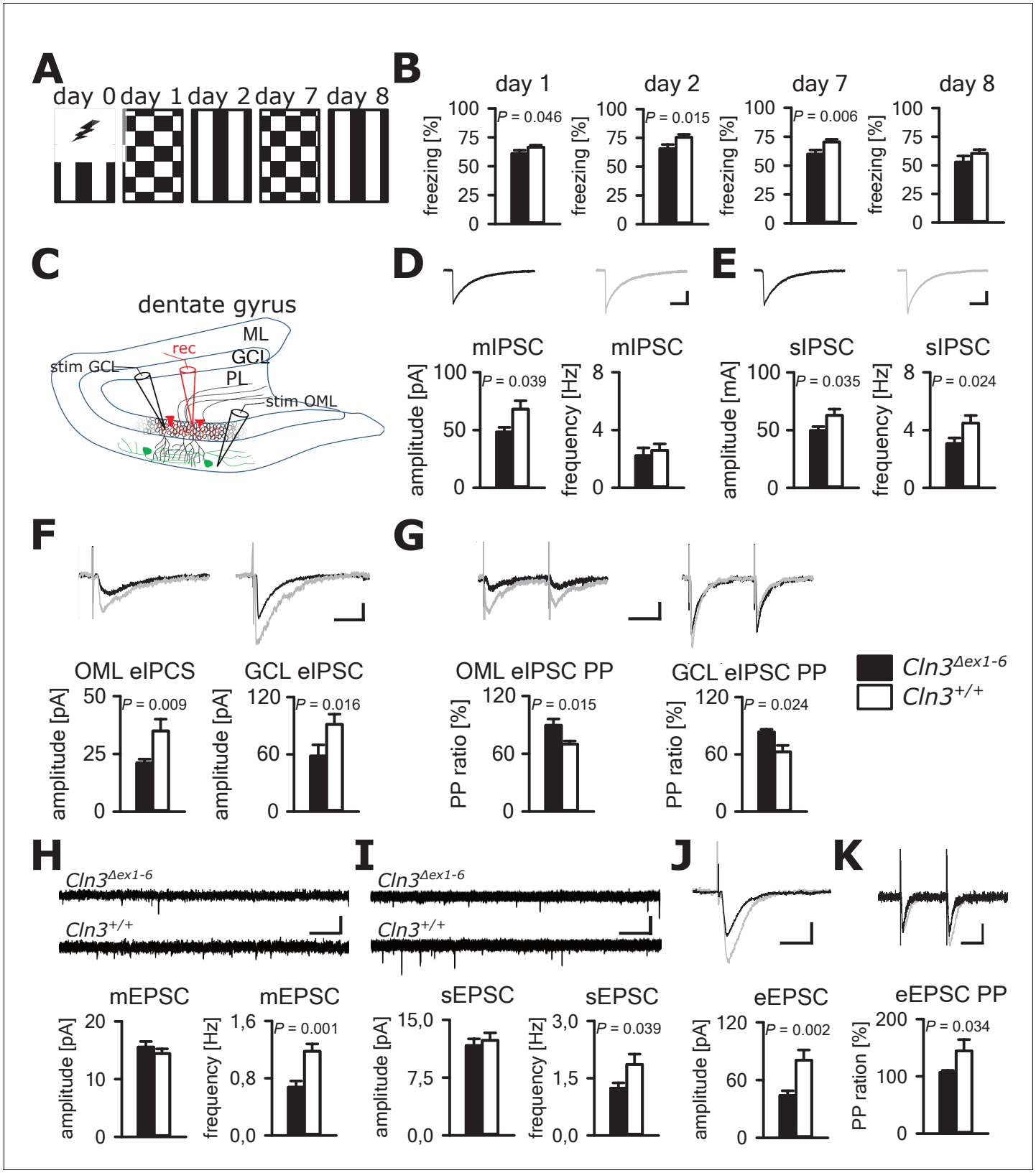

Figure 4. Learning deficits and disturbed hippocampal synaptic transmission in *Cln3*$^{\Delta ex1-6}$ mice at the age of 14 months. (**A**) For induction of fear conditioned and contextual learning a conditioned acoustic stimulus (tone) was paired with an unconditioned stimulus (electric shock) on day 0 in a specific environment (schematically illustrated as black and white stripes). On days 1 and 7, the conditioned stimulus was presented in a 'novel'

Figure 4 continued on next page

Figure 4 continued

environment (chequered pattern) to test conditioned fear learning. Contextual fear learning was tested on days 2 and 8 by presenting the same environment as on day 0 without the conditioned stimulus (tone). (**B**) Rehearsal of cued and context learning was impaired in *Cln3*$^{\Delta ex1\text{-}6}$ mice. Reduced freezing of *Cln3*$^{\Delta ex1\text{-}6}$ mice was detected on day 1 and day 7 (auditory cue in novel environment) and day 2 (conditioned environment without auditory cue) (n = 18 vs.23; Student's t-test). On day 8 both groups showed a reduction of contextual fear behavior without significant differences. (**C**) Schematic illustration of the patch-clamp recording situation in the hippocampal dentate gyrus (rec, shown in red). Stimulation electrodes (stim) were positioned in the granule cell layer (GCL) and outer part of the molecular layer (OML) to stimulate GABAergic efferents of different interneuron subtypes (PL: polymorphic layer). For recording of evoked excitatory postsynaptic currents stimulation was performed in the OML to stimulate the lateral perforant pathway (LPP). (**D**) Analysis of GABAergic mIPSC in presence of TTX revealed reduction of the peak amplitude, whereas the frequency was unchanged (example traces from a single neuron are shown in the upper panel; in grey: traces of a wt mouse, in black: traces of a *Cln3*$^{\Delta ex1\text{-}6}$ mouse; wt: n = 11 cells from nine mice; *Cln3*$^{\Delta ex1\text{-}6}$: n = 10/8; Student's t-test; scale bar: 10 ms / 20 pA). (**E**) Frequency and peak amplitude of sIPSC were significantly reduced in dentate gyrus GC of *Cln3*$^{\Delta ex1\text{-}6}$ mice; wt: n = 14/11; *Cln3*$^{\Delta ex1\text{-}6}$: n = 14/11; amplitude: Student's t-test; frequency: Mann-Whitney test; scale bar: 10 ms / 20 pA). (**F**) Minimal threshold stimulation of afferents was performed in the OML and the GCL to obtain eIPSC of individual afferents projecting from different hippocampal areas. In slices of *Cln3*$^{\Delta ex1\text{-}6}$ mice eIPSC derived from both stimulation sites showed reduced peak amplitude in comparison to wt littermates (OML: n = 11/11 vs. 11/11, GCL: n = 12/8 vs. 10/7; Student's t-test; scale bar: 25 ms / 10 pA). (**G**) Paired pulse depression as a characteristic feature of presynaptic short-term plasticity in the synapses on dentate gyrus GC was affected in *Cln3*$^{\Delta ex1\text{-}6}$ mice at both stimulation sites (OML: n = 10/10 vs. 11/11; GCL: n = 12/8 vs. 8/7; Student's t-test; scale bar: 50 ms / 10 pA). (**H and I**) miniature (**m**) EPSC frequency (**H**, wt: n = 15/7 vs. *Cln3*$^{\Delta ex1\text{-}6}$: n = 11/6; amplitude: Mann-Whitney test; frequency: Student's t-test) and spontaneous (s) EPSC frequency was reduced in the dentate gyrus GC in *Cln3*$^{\Delta ex1\text{-}6}$ mice (**I**, wt: n = 14/7; *Cln3*$^{\Delta ex1\text{-}6}$: n = 17/6; Mann-Whitney test; scale bars 20 pA and 500 ms). (**J**) The amplitude of eEPSC was reduced at high stimulation intensities (wt: n = 12/7; *Cln3*$^{\Delta ex1\text{-}6}$: n = 12/6; Student's t-test; scale bars 40 pA and 50 ms). (**K**) The paired-pulse facilitation of the LPP eEPSC at 100 ms interstimulus interval was reduced in *Cln3*$^{\Delta ex1\text{-}6}$ mice (wt: n = 12/7; *Cln3*$^{\Delta ex1\text{-}6}$: n = 12/6; Student's t-test; scale bars 50 pA and 50 ms). Exact p values, dispersion and precision measures are provided in ***Supplementary file 2***.

DOI: https://doi.org/10.7554/eLife.28685.009

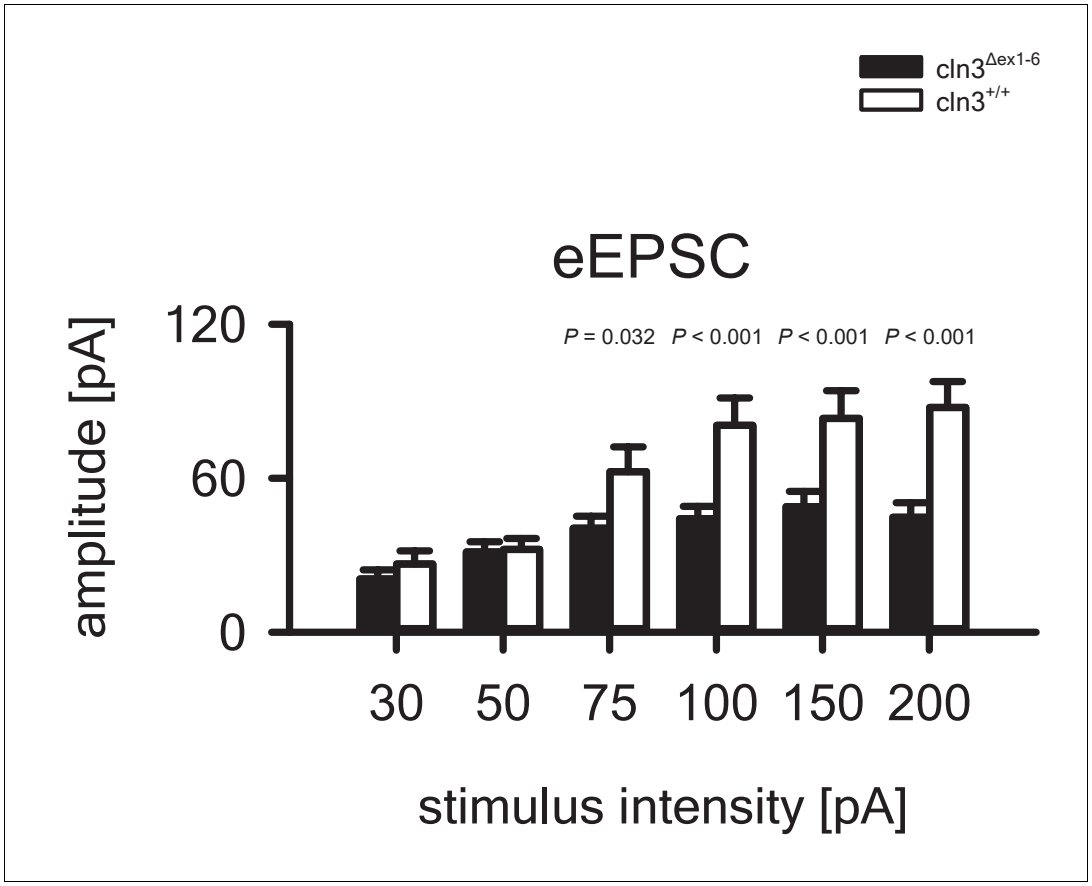

Figure 4—figure supplement 1. Reduced eEPSC amplitudes in the hippocampus of 14 months old *Cln3*$^{\Delta ex1\text{-}6}$ mice. The amplitude of eEPSCs in *Cln3*$^{\Delta ex1\text{-}6}$ mice is reduced at stimulation intensities ≥ 75 pA but is unchanged at stimulation intensities in the range of minimal stimulation (wt: n = 12/7; *Cln3*$^{\Delta ex1\text{-}6}$: n = 12/6; Student's t-test). Exact values for N, dispersion and precision measures are provided in ***Supplementary file 2***.

DOI: https://doi.org/10.7554/eLife.28685.010

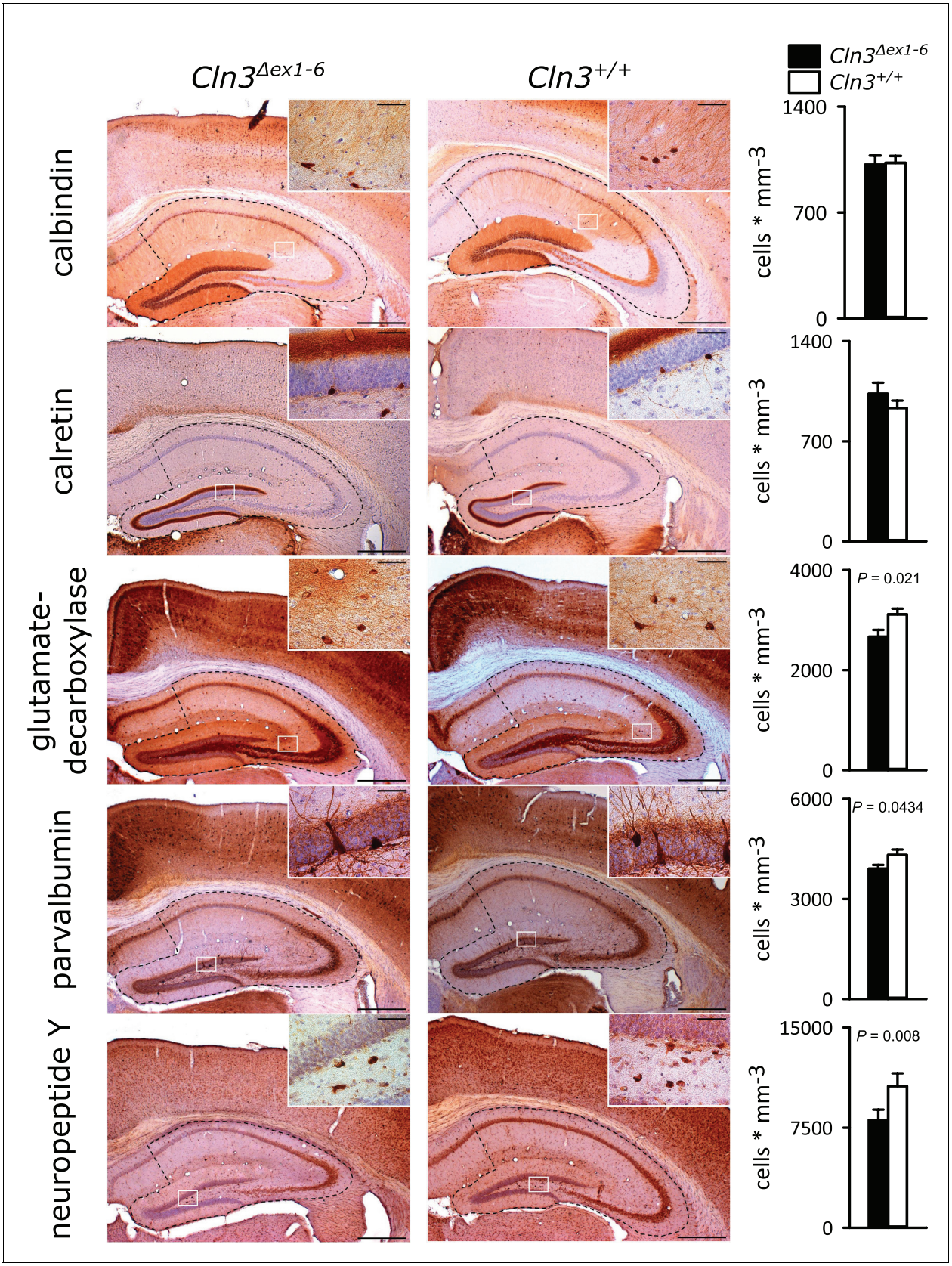

Figure 5. Loss of GABAergic interneurons in the hippocampus of *Cln3*$^{\Delta ex1-6}$ mice at the age of 14 months. Quantitative stereological analysis of interneuron subclasses revealed a reduced number of parvalbumin, neuropeptide Y and GAD-positive interneurons, whereas other markers were

Figure 5 continued on next page

Figure 5 continued

unchanged. Note that GAD-positive cells were not counted in the hilus of the dentate gyrus since here intense staining of the fiber network precluded precise cell differentiation (scale bar: 500 μm; inset: 50 μm; *n = 13 to 16*)). Exact values of N, dispersion and precision measures are provided in ***Supplementary file 2***.

DOI: https://doi.org/10.7554/eLife.28685.011

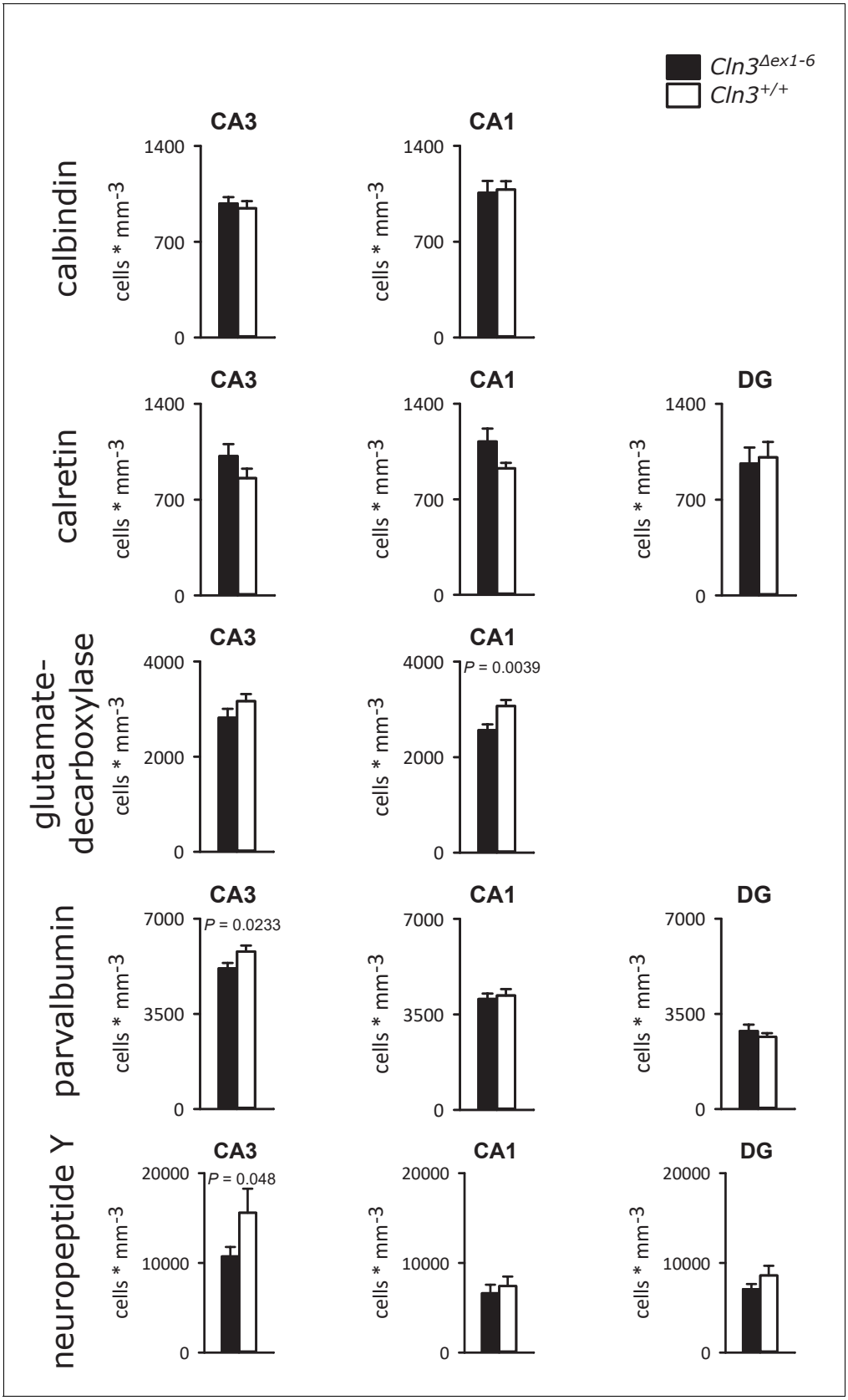

Figure 5—figure supplement 1. Density of interneurons within the hippocampal subfields of *Cln3*$^{\Delta ex1-6}$ mice and wt littermates. Analysis of interneuron density within hippocampal subfields revealed a reduction of GAD in the CA1 region of *Cln3*$^{\Delta ex1-6}$ mice (n = 17 vs. 14; Student's t-test) and a reduction

Figure 5—figure supplement 1 continued on next page

Figure 5—figure supplement 1 continued

of parvalbumin (n = 17 vs. 14; Student´s t-test) and NPY-positive cells (n = 17 vs. 14, Mann-Whitney test) in CA3 region. The density of calbindin and calretinin-positive cells was unchanged in all hippocampal subfields. Exact values of N, dispersion and precision measures are provided in ***Supplementary file 2***.

DOI: https://doi.org/10.7554/eLife.28685.012

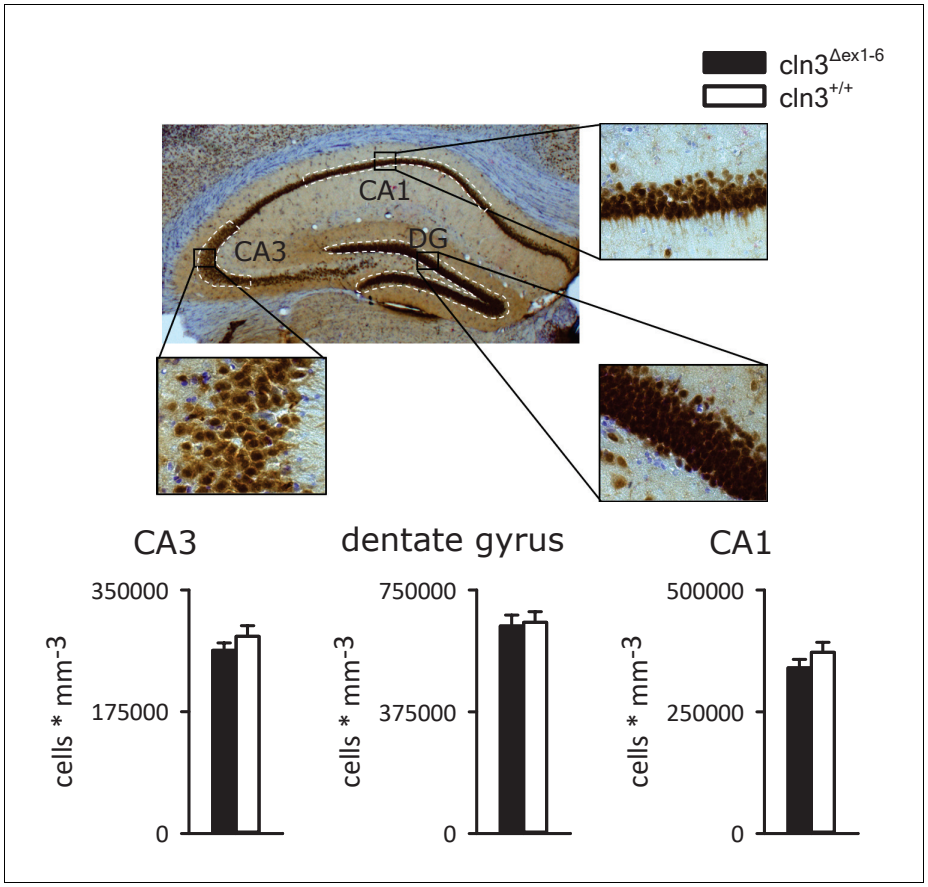

Figure 5—figure supplement 2. Density of NeuN-positive cells is unchanged in the hippocampus of 14-month-old *Cln3*$^{\Delta ex1-6}$ mice. NeuN-positive neurons were analyzed in the principal cell layers of the hippocampus. Stereological analysis revealed unchanged count of NeuN-positive cells in the dentate gyrus and in the CA1 and CA3 subfield of the hippocampus (n = 9 vs. 8). Exact p values, dispersion and precision measures are provided in ***Supplementary file 2***.

DOI: https://doi.org/10.7554/eLife.28685.013

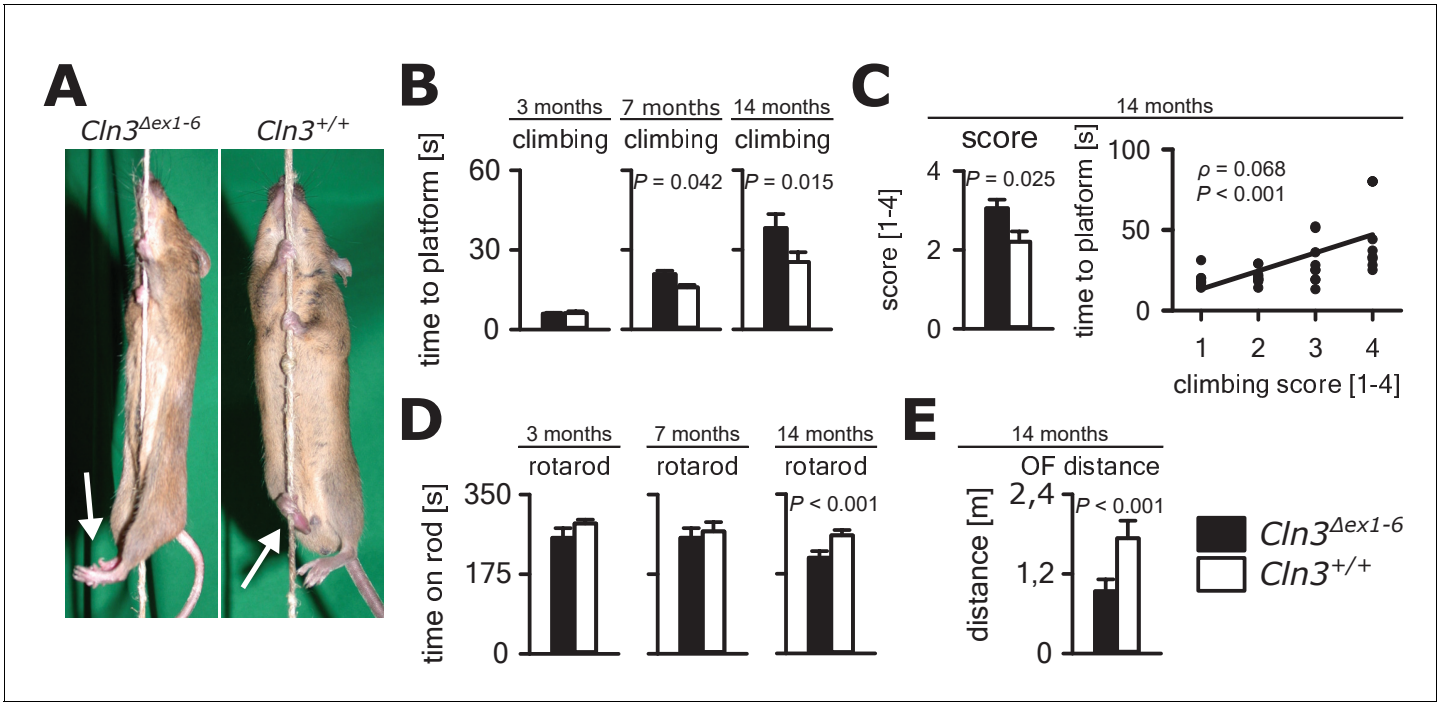

Figure 6. Progressive ataxia and motor impairment in *Cln3*$^{\Delta ex1-6}$ mice. (**A, B**) Mice were trained to climb a vertically stretched cord of 1 m length to reach a platform (climbing test). Mice used their limbs in an alternating manner that allows fast movement and rapid climbing (see also ***Video 1***). Time to platform of 3 months old *Cln3*$^{\Delta ex1-6}$ mice was unchanged to wt littermates. At later time points, *Cln3*$^{\Delta ex1-6}$ mice developed an abnormal climbing pattern leading to prolonged climbing time at the age of 7 months (n = 17 vs. 18, Mann-Whitney test) and more pronounced at an age of 14 months (n = 17 vs. 19, Mann-Whitney test). Moreover, *Cln3*$^{\Delta ex1-6}$ mice showed ataxic limb movements that led to difficulties in grasping the rope (arrows in A). (**C**) The coordination of hind limb movement was significantly impaired in *Cln3*$^{\Delta ex1-6}$ mice at 14 months as assessed by the climbing score evaluating hind limb use and correlated with the time needed to reach the platform (n = 17 vs. 19, Mann-Whitney test; Spearman's rank correlation coefficient ρ = 0.68). (**D**) Motor performance tested on the RotaRod revealed deficits of forced walking behavior in *Cln3*$^{\Delta ex1-6}$ mice at 14 months when compared to age-matched wt littermates (3 months: n = 12 vs. 18; 7 months: n = 13 vs. 18, both Mann-Whitney test; 14 months: n = 17 vs. 21, Student's t-test). (**E**) In the OF the total walking distance was reduced in 14 month old *Cln3*$^{\Delta ex1-6}$ mice (n = 18 vs. 20, Mann-Whitney test). Exact dispersion and precision measures are provided in ***Supplementary file 2***.

DOI: https://doi.org/10.7554/eLife.28685.014

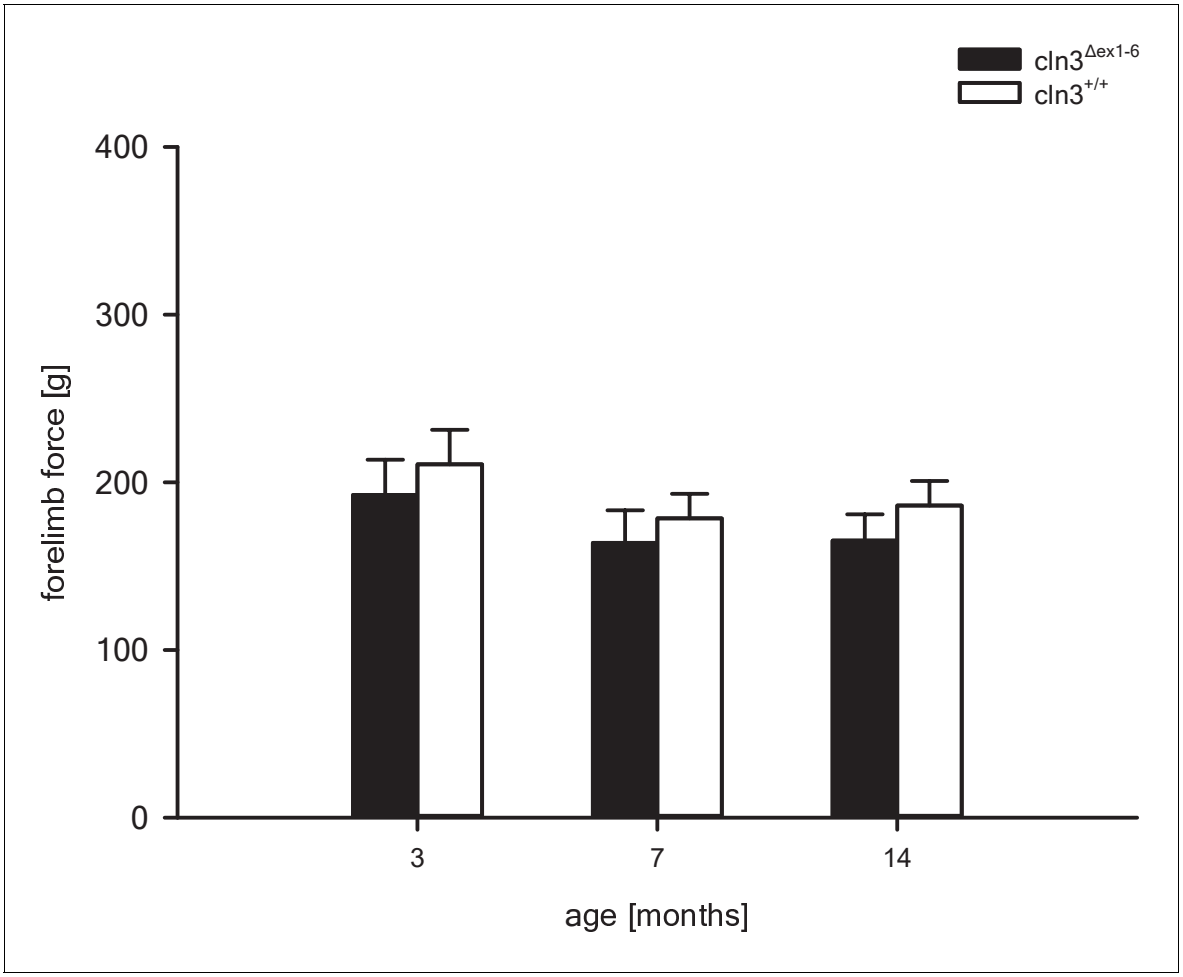

Figure 6—figure supplement 1. Grip strength of *Cln3*$^{\Delta ex1\text{-}6}$ mice and wt littermates at different ages. Grip strength of the forelimbs is not affected in *Cln3*$^{\Delta ex1\text{-}6}$ mice. Grip strength measures of wt and *Cln3*$^{\Delta ex1\text{-}6}$ mice were unchanged between genotypes at all time points (3 months: n = 11 vs. 12; 7 months: n = 13 vs. 13; 14 months n = 22 vs. 18). Exact p values, dispersion and precision measures are provided in ***Supplementary file 2***.
DOI: https://doi.org/10.7554/eLife.28685.015

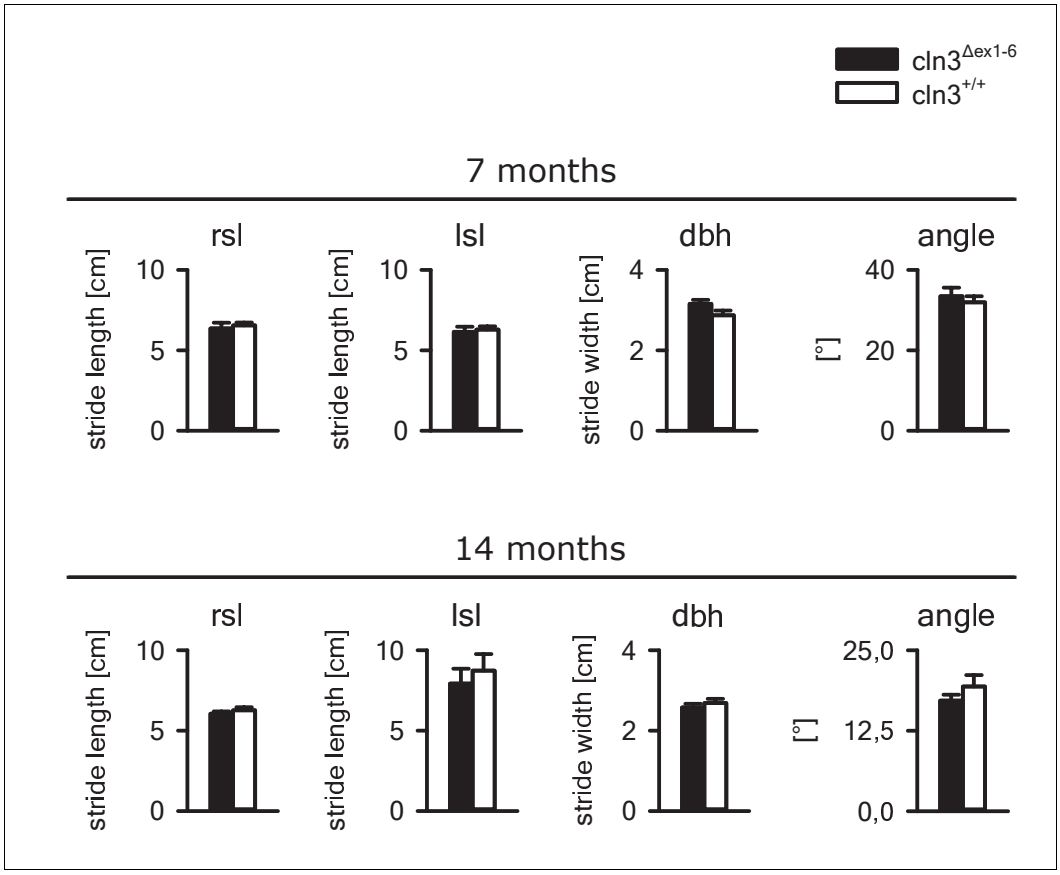

Figure 6—figure supplement 2. Gait analysis of *Cln3*$^{\Delta ex1-6}$ mice and wt littermates. Gait analysis of *Cln3*$^{\Delta ex1-6}$ mice at the age of 7 and 14 months revealed no differences as compared to wt mice. Right and left stride length (rsl and lsl), distance between hind feet (dbh) and angle between hindfeet were not affected in *Cln3*$^{\Delta ex1-6}$ mice (7 and 14 months: n = 10 vs. 10). Exact p values, dispersion and precision measures are provided in ***Supplementary file 2***.

DOI: https://doi.org/10.7554/eLife.28685.016

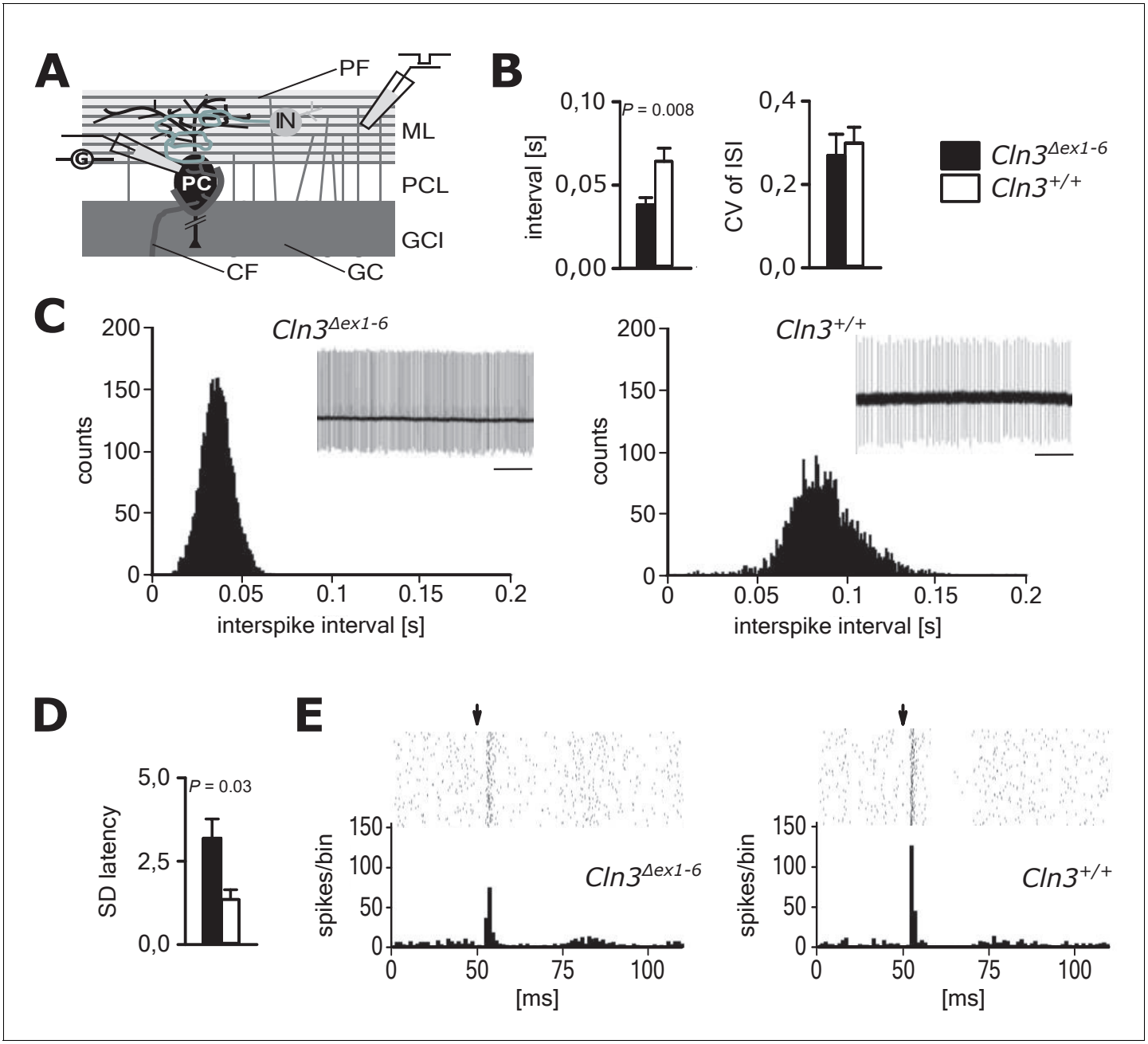

Figure 7. Pathological firing of cerebellar Purkinje cells (PC) of *Cln3*$^{\Delta ex1-6}$ mice at the age of 14 months. (**A**) Schematic drawing of neurons and connections in the cerebellar cortex. Spontaneous and evoked action potentials of PC were recorded in loose patch configuration. Granule cells (GC) give rise to the parallel fibers (PF) which excite PC and local interneurons (IN). IN induce feed forward inhibition onto PC (CF = climbing fiber; GCL = granule cell layer; ML = molecular layer; PCL = Purkinje cell layer). (**B**) Inter-spike intervals of spontaneous action potential firing were reduced in *Cln3*$^{\Delta ex1-6}$ mice while the regularity of spiking (CV ISI) was unchanged (n = 12 cells from 8 mice vs. 12/6, Student's t-test). (**C**) Histograms of inter-spike intervals of spontaneous activity and representative recordings (upper right inset, scale bar: 500 ms) are shown. Inter-spike intervals were reduced and shifted to smaller bin sizes in *Cln3*$^{\Delta ex1-6}$ mice. (**D**) The standard deviation of the latency of the first action potential after parallel fiber stimulation was increased in *Cln3*$^{\Delta ex1-6}$ indicating enhanced jitter of PC firing upon PF activation (n = 12/8 vs. 13/6, Mann-Whitney test). (**E**) Representative raster plots and histograms showing PC simple spikes upon single stimulation of parallel fibers. Each horizontal series of points in the raster plot represents an individual recording. Arrows indicate onset of stimulation after baseline recording of 50 ms. In the example of a wt mouse stimulation elicited simple spikes in a narrow time window and a clear spiking pause following the initial response, while in the *Cln3*$^{\Delta ex1-6}$ mouse the jitter of firing after PF stimulation is increased and the spiking pause is reversed. Exact dispersion and precision measures are provided in ***Supplementary file 2***.

DOI: https://doi.org/10.7554/eLife.28685.018

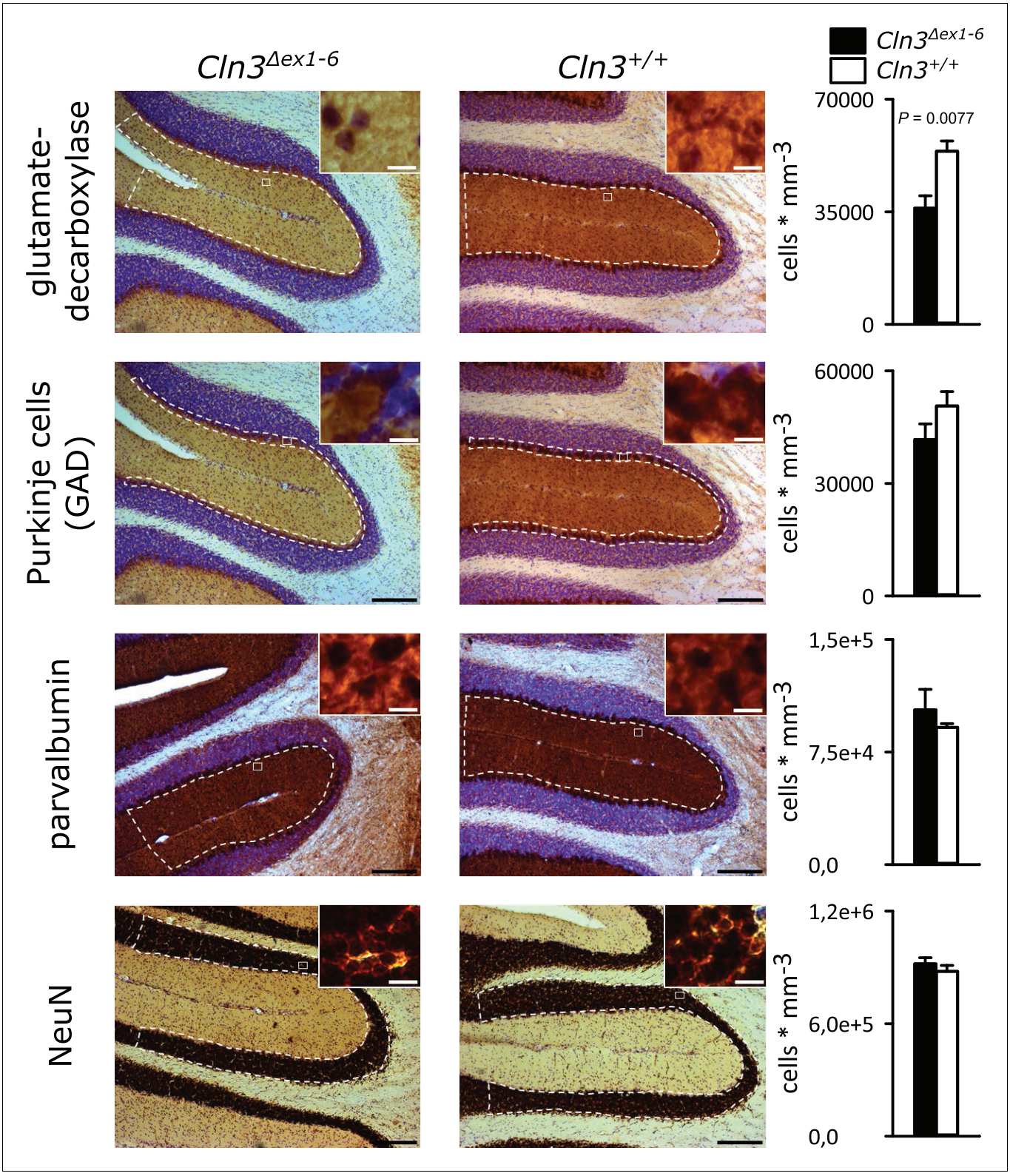

Figure 8. Reduction of GAD-positive interneurons in the cerebellar molecular layer of 14 months old *Cln3*$^{\Delta ex1-6}$ mice. Quantitative stereological analysis of interneuron subclasses and NeuN-positive neurons in coronar cerebellar slices revealed a reduced number of GAD-positive interneurons within the molecular layer (ML) (n = 9 vs. 8, Student's t-test) whereas other markers as well as the number of Purkinje cells were unchanged (scale bar: 200 µm; inset: 10 µm). Exact values of N, dispersion and precision measures are provided in ***Supplementary file 2***.

DOI: https://doi.org/10.7554/eLife.28685.019

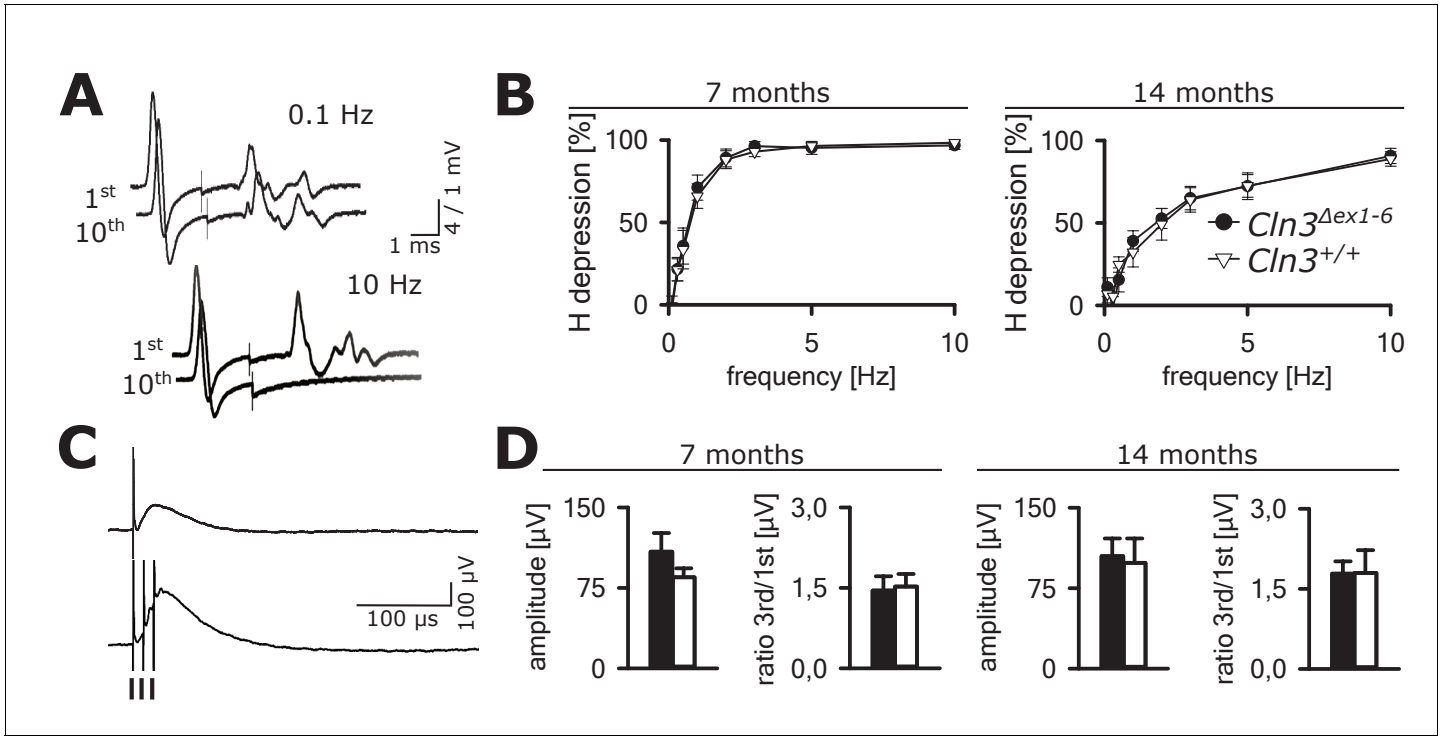

Figure 9. Spinal networks are unaffected in *Cln3*$^{\Delta ex1\text{-}6}$ mice. (**A**) Example traces for H-Reflex recordings in mice; the first major deflection is the motor response (M-wave) upon anterograde sciatic nerve stimulation, the second is the H-Reflex after monosynaptic transmission in the spinal cord followed by a polyphasic F-wave.1st and 10th trace of 10 consecutive stimuli are shown for the indicated frequencies. Note that H-Reflex amplification is fourfold higher than for the M-wave. The H-Reflex is unchanged after 10 serial stimuli at 0.1 Hz stimulation, whereas it is completely abolished (100% depression) after 10 stimuli at 10 Hz (post-activation depression, primarily mediated by local GABAergic interneurons). (**B**) Post-activation depression of the H-Reflex in *Cln3*$^{\Delta ex1\text{-}6}$ and wt mice was tested at the age of 7 and 14 months and was unchanged at both time points at all investigated stimulation frequencies. Note, that the depression of H-Reflex is shifted to higher frequencies in both genotypes at higher age of 14 months, indicating age-dependent changes within the spinal networks in both groups (7 months n = 12 recordings from 10 mice vs. 14/13, 14 months n = 16/10 vs. 13/8; Two-way ANOVA). (**C**) Example traces for recordings of dorsal root potentials (DRP) in mice in-vivo as a direct measurement of spinal GABAergic presynaptic inhibition. The upper trace shows a recording of the DRP after a single stimulus, the lower trace shows the DRP after three stimuli demonstrating temporal summation. Arrows indicate electric stimulations. (**D**) Peak amplitudes of DRP after a single stimulus and the ratio of peak amplitudes after time-dependent summation vs. single stimulation are not significantly different in *Cln3*$^{\Delta ex1\text{-}6}$ and wt mice at both analyzed time points indicating unchanged spinal presynaptic inhibition (7 months n = 14 recordings from 8 mice vs. 17/8, 14 months n = 17/9 vs. 10/6). Exact p values, dispersion and precision measures are provided in ***Supplementary file 2***.

DOI: https://doi.org/10.7554/eLife.28685.020

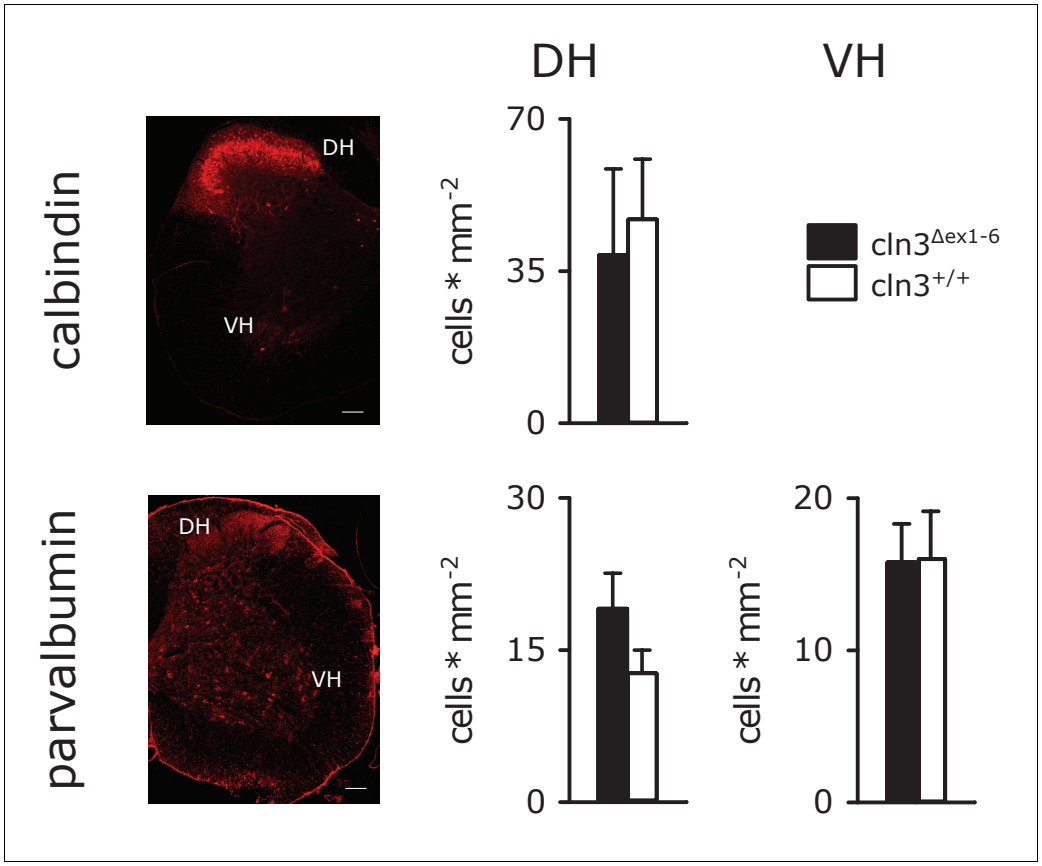

Figure 9—figure supplement 1. Number of spinal cord interneurons are unaffected. Quantitative analysis of parvalbumin- and calbindin-positive interneurons showed no difference of cell counts in the ventral (VH) or dorsal horn (DH) of the spinal cord in of wt and *Cln3*$^{\Delta ex1-6}$ mice (n = 6 vs. 7; scale bar: 50 μm). Exact p values, dispersion and precision measures are provided in ***Supplementary file 2***.

DOI: https://doi.org/10.7554/eLife.28685.021